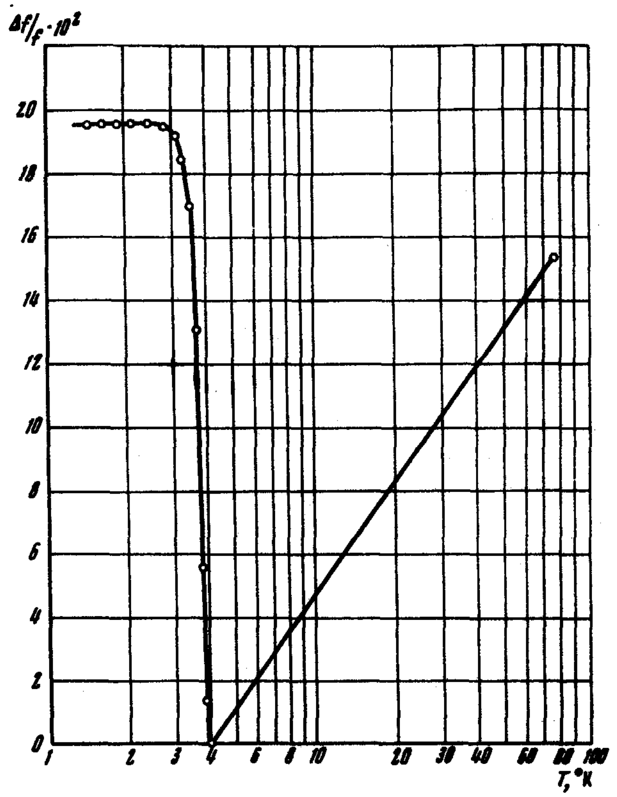

Fig. 3. Measured temperature dependence of the relative change of the autodyne frequency for single-crystal TbF_3.

Unlike in the ethyl sulfate, we did observe in the terbium trifluoride single crystal a magnetic ordering at 3.9°K. We plotted the temperature dependence of the frequency of the autodyne generator used as the NMR pickup (Fig. 3). The high-temperature region is described by a Curie law with a constant $C_0 = 1.9$. Near 4°C, a sharp change in the frequency takes place and corresponds to the transition to the antiferromagnetic state, after which the frequency ceases to change. Similar changes are described in the papers by the Leiden Group [3]. An additional confirmation of the magnetic ordering is the study of the NMR of F^{19} in TbF_3. A single line with a recorded signal/noise ratio equal to 3 is observed at 4.2°K. When the temperature is lowered at 1.5°K, this ratio increases by several orders of magnitude.

More detailed results of the research will be published later.

The authors thank B.I. Kochelaev and R.A. Dautov for valuable advice and discussions.

[1] A.A. Abragam and B. Bleaney, Electron Paramagnetic Resonance of Transition Ions, Oxford University Press, 1970.
[2] J.M. Baker, J. Phys. C. Solid State Phys. 4, 1631 (1971).
[3] K.W. Mess, E. Lagendijk, D.A. Curtis, and W.J. Huiskamp, Physica 34, 126 (1967).

INFLUENCE OF SPECTRAL LINE WIDTH OF EXCITING RADIATION ON THE GAIN IN STIMULATED SCATTERING

A.Z. Grasyuk, I.G. Zubarev, and N.V. Suyazov
P.N. Lebedev Physics Institute, USSR Academy of Sciences
Submitted 13 July 1972
ZhETF Pis. Red. 16, No. 4, 237 - 240 (20 August 1972)

1. The amplification of the light in stimulated scattering in a pump field of intensity I_p (W/cm^2) in an active medium of length L (cm) is proportional to $\exp(gI_pL)$. The gain g (cm/W) is given by $g = A/\Delta\omega$, where $\Delta\omega = 2\pi(\Delta\nu_p + \Delta\nu_{sp})$, while $\Delta\nu_p$ (cm^{-1}) and $\Delta\nu_{sp}$ (cm^{-1}) are respectively the widths of the spectral lines of the exciting radiation and of the spontaneous scattering. For stimulated Raman scattering (SRS) we have $A = \lambda_S^2\sigma N/Y$, where λ_S is the wavelength of the first Stokes component, σ is the SRS cross section, and N is the concentration of the molecules. For stimulated Mandel'shtam-Brillouin scattering $A = \gamma^2k^2/(n^3c\rho v)$, where γ is the photoelastic constant of the medium, ρ is its den-

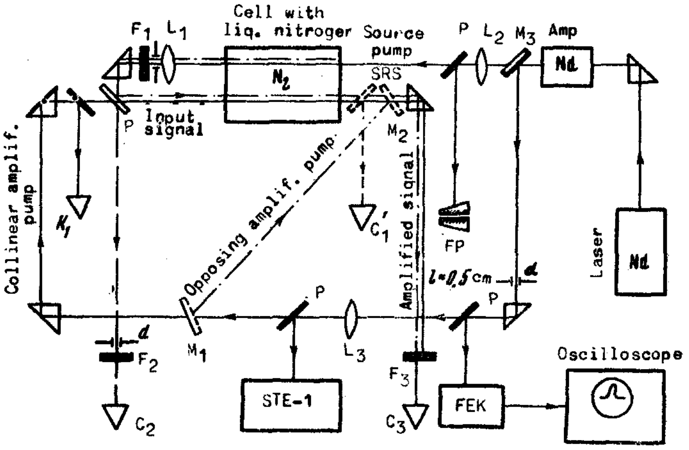

Fig. 1. Block diagram of experimental setup: $C_1 - C_3$) calorimeters; $F_1 - F_3$) selective filters passing the Stokes signal and cutting of the pump radiation. P) plane-parallel glass plates; FP) Fabry-Perot interferometer with 0.5 cm gap; STE-1) spectrograph; FEK) coaxial photocell with I2-7 oscilloscope; Nd) Q-switched laser using phosphate neodymium glass; Amp) Nd-glass amplifier; solid line) pump; dash-dot line) SRS signal; dashed line) part of the system used to investigate the opposing variant of the Stokes amplifier.

density, n is the refractive index, $k = 2\pi/\lambda$ is the wave vector, and c and v are the speeds of the light and of the hypersound, respectively.

In the case of broadband pumping, when $\Delta\nu_p >> \Delta\nu_{sp}$, one would expect the gain g to decrease always with increasing $\Delta\nu_p$: $g \simeq A/\Delta\nu_p$. Our earlier experiments [1], however, have shown for the first time that this is not so. It turned out that under certain conditions the efficiency of conversion into the Stokes component of the SRS (determined by the gain) may be independent of the pump spectral line width when the latter ranges from 10^{-3} to 40 cm^{-1}.

Various singularities of the stimulated scattering in a broad-band pumping field (SBBS) were subsequently examined in theoretical papers [2, 3], where new effects were predicted.

In the experiments described here we have observed new phenomena which have been predicted theoretically in [3] and appear at pump intensities commonly used in practical applications. These new phenomena are asymmetry with respect to the "front-back" directions, and a threshold dependence of the gain increment on the excitation intensity in SBBS.

We investigated experimentally the dependence of the increment of the SRS gain on the pump intensity for different ratios of $\Delta\nu_p$ and $\Delta\nu_{sp}$ in two amplification variants, collinear and opposing (the pump and the external signal have equal and opposing directions, respectively).

The pump source was a Q-switched phosphate-neodymium-glass laser. Its spectrum was regulated in the range from $\Delta\nu_p \lesssim 3 \times 10^{-2}$ cm^{-1} (Q-switching with a dye) to $\Delta\nu_p = 0.3$ cm^{-1} (Q-switching with a rotating prism and mode selection: two plane-parallel glass plates of unequal thickness as the output mirror of the resonator).

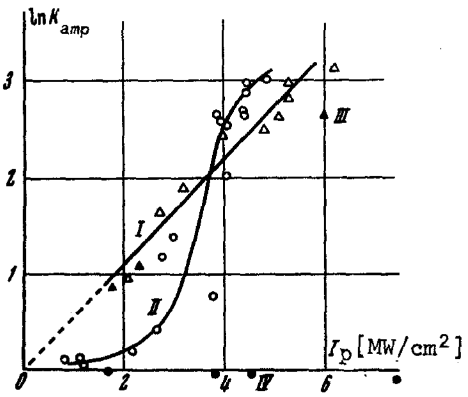

Fig. 2. Experimental plots of $\ln K_{amp} = \ln[E_S^{out}/E_S^{in}]$ vs. the pump intensity I_p for the collinear and opposing amplification variants. Light symbols - collinear variant, dark symbols - opposing variant; triangles - $\Delta\nu_p \leq 0.03$ cm^{-1}, circles - $\Delta\nu_p = 0.3$ cm^{-1}.

For liquid nitrogen, $\Delta\nu_{sp} = 0.067$ cm^{-1} and the broadband condition $\Delta\nu_p \gg \Delta\nu_{sp}$ was satisfied at $\Delta\nu_p = 0.3$ cm^{-1}. At the same time, the pump threshold intensity $I_p^{thr} = (2\pi\nu'/g_0)\Delta\nu_p$, noted in [3], turns out to be too small. Here $\nu' = |(v_S - v_p)/\bar{v}|$ is the relative dispersion of the pump group velocities (v_p) and the Stokes component (v_S) ($\nu' \sim 10^{-2}$ and $\nu' = 2$ in the case of collinear and opposing amplification, respectively), and g_0 is the gain in narrow-band excitation, $g_0 = 10^{-2}$ cm/MW for liquid nitrogen. This means that in the case of collinear amplification we have $I_p^{thr} \approx 1.8$ MW/cm. Also eliminated are such undesirable side effects as self-focusing, noticeable conversion into the Stokes component in the exciting beam without an external signal1), etc. For opposing amplification, $I_p^{thr} \approx 300$ MW/cm^2.

A block diagram of the experimental setup is shown in Fig. 1. The neodymium-laser radiation is split by mirror M_3 into two beams. One of them is focused by lens L_2 and produces in the cell SRS whose first Stokes component is used as the input signal for the SRS amplifier. The gain was measured with calorimeters C_2 and C_3; the shape and duration of the pump pulse was registered with a coaxial photocell FEK-09 and an I2-7 oscilloscope. The spectral composition of the radiation was monitored with an STE-1 spectrograph and a Fabry-Perot interferometer with gap 0.5 cm (resolution 0.03 cm^{-1}).

3. We measured in the experiment the quantity $\ln K_{amp} = \ln[E_S^{out}/E_S^{in}]$ as a function of the pump intensity I_p at a fixed length of the amplifier cell $L = 50$ cm. Here E_S^{in} and E_S^{out} are the energies of the Stokes signals on entering and leaving the amplifier cell, respectively ($E_S^{in}, E_S^{out} \ll I_p\tau_p$). Thus, the deviation of $\ln K_{amp}$ from linearity in I_p ($\ln K_{amp} = gI_pL$) offers evidence of the change of the value of the gain g.

The experimental results are shown in Fig. 2. We see that in the case of narrow-band pumping (plots I and III) the corresponding narrow-band gain g_0 is practically constant ($g_0 \approx 10^{-2}$ cm/MW) and does not depend on the direction of the mutual propagation of the pump and signal.

An entirely different picture is observed in the case of broadband excitation (II, IV). In the collinear case (II), so long as the pump intensity is lower than a certain threshold ($I_p^{thr} \approx 3$ MW/cm^2), the "broadband" gain g_{br} is much lower than the narrow-band gain ($g_{br} < g_0$). With increasing excess over threshold, g_{br} increases sharply and approaches g_0. In other words, the gain

---

1) In this case it was observed that $I_p > 6 - 8$ MW/cm^2.

becomes the same as for narrow-band pumping. In the opposing variant, there is no gain at all in the entire region of investigated intensities ($g_{br} \simeq 0$). This fact has not yet been theoretically explained.

The authors are grateful to Yu.E. D'yakov and S.A. Akhmanov for fruitful discussions of this question, to V.G. Smirnov and V.I. Mishin for a useful discussion of the organization of the experiments, and to V.V. Bocharov for help with the experiments.

[1] V.V. Bocharov, A.Z. Grasyuk, I.G. Zubarev, and V.F. Mulikov, Zh. Eksp. Teor. Fiz. 56, 430 (1969) [Sov. Phys.-JETP 29, 235 (1969)].
[2] Yu.E. D'yakov, ZhETF Pis. Red. 11, 362 (1970) [JETP Lett. 11, 243 (1970)].
[3] S.A. Akhmanov, Yu.E. D'yakov, and A.S. Chirkin, ibid. 13, 724 (1971) [13, 514 (1971)].
[4] V.V. Bocharov, M.G. Gangardt, A.Z. Grasyuk, I.G. Zubarev, and E.A. Yukov, Zh. Eksp. Teor. Fiz. 57, 1585 (1969) [Sov. Phys.-JETP 30, 858 (1970)].

2.5 MEGABAR PRESSURE IN ANVILS MADE OF CARBONADO TYPE DIAMOND

L.F. Vereshchagin, E.N. Yakovlev, G.N. Stepanov, K.Kh. Bibaev, and B.V. Vinogradov
Institute of High Pressure Physics
Submitted 14 July 1972
ZhETF Pis. Red. 16, No. 4, 240 - 242 (20 August 1972)

In his 1941 paper on the limit of usable pressures [1], Bridgman cites data on pressures obtained between a truncated cone and a plane made of a hard alloy (carboloy 905).

Since 1941, the properties of hard materials based on tungsten carbide (carboloy, VK alloys), have been continuously improved, but no substantial progress was made in such experiments.

In the cited paper, Bridgman [1] expressed the opinion that much higher contact pressures might be obtained by using a material consisting of microscopic diamond grains firmly bonded to one another. Natural diamond fine-grain aggregates, in Bridgeman's opinion, do not satisfy these requirements because of their porous structure.

In 1969, we reported the synthesis of diamonds of the carbonado type [2]. Carbonado is a polycrystalline formation made up of microscopic diamond grains that are firmly bonded with one another.

We prepared a cone and a plane of carbonado. The cone had a vertex angle 168° and the vertex was somewhat flattened. The diamond plane and cone were placed in a steel mount.

The average contact pressure P was calculated from the formula

$$P = \frac{F}{S}$$

where F is the applied force and S the area on which the force was applied.

The force was measured with a calibrated dynamometer. The area on which the force F was concentrated was determined from the print produced on a film deposited on the surface of the diamond plane.